Accepted Manuscript

Anaerobic Conversion of Hydrogen and Carbon Dioxide to Fatty Acids Production in a Membrane Biofilm Reactor: A Modeling Approach

Xueming Chen, Bing-Jie Ni

PII: S1385-8947(16)31123-8
DOI: http://dx.doi.org/10.1016/j.cej.2016.08.049
Reference: CEJ 15615

To appear in: *Chemical Engineering Journal*

Received Date: 3 June 2016
Revised Date: 8 August 2016
Accepted Date: 9 August 2016

Please cite this article as: X. Chen, B-J. Ni, Anaerobic Conversion of Hydrogen and Carbon Dioxide to Fatty Acids Production in a Membrane Biofilm Reactor: A Modeling Approach, *Chemical Engineering Journal* (2016), doi: http://dx.doi.org/10.1016/j.cej.2016.08.049

Anaerobic Conversion of Hydrogen and Carbon Dioxide to Fatty Acids Production in a Membrane Biofilm Reactor: A Modeling Approach

Xueming Chen, Bing-Jie Ni*

Advanced Water Management Centre, The University of Queensland, St. Lucia, Brisbane, QLD 4072, Australia

*Corresponding author:

Dr. Bing-Jie Ni

Advanced Water Management Centre

The University of Queensland

Australia

Phone: + 61 7 3346 3230

Fax: +61 7 3365 4726

E-mail: b.ni@uq.edu.au

ABSTRACT

Biological conversion of gaseous compounds (e.g., H_2/CO_2) into valuable liquid fuels or chemicals using mixed culture is a promising technology, which could be effectively and efficiently implemented in a membrane biofilm reactor (MBfR) with gas being supplied from inside of membranes. In this study, a model integrating multiple production pathways of fatty acids (including acetate, butyrate, and caproate) was developed and tested using reported mixed culture experimental data from a lab-scale MBfR fed with 60% H_2 and 40% CO_2. The uncertainty of the four estimated model parameters was explored by a sensitivity analysis. With the developed model, the impacts of key process parameters (i.e., gas supply and hydraulic retention time (HRT)) on the performance of the MBfR converting H_2/CO_2 to fatty acids were then investigated. The results show that a high HRT is imperative for chain elongation to produce a higher proportion of caproate with a higher added value. A proper gas supply should be provided to favour the speciation of biological gas conversion products as well as to fully exploit the conversion capacity of the MBfR. The findings of this work provide useful information for a better understanding and further applications of this MBfR technology for mixed culture syngas fermentation.

KEYWORDS: fatty acids; mixed culture; hydrogen; carbon dioxide; membrane biofilm reactor; mathematical modelling

INTRODUCTION

While anaerobic digestion of organic wastes mainly aims at methane production, there has been substantial emergence that focuses on more targeted reactions to generate biomaterials of higher value [1], such as fatty acids, ethanol, and butanol. The produced short-chain fatty acids (acetate (C2) and butyrate (C4)) are important precursors for biofuel

production [2-4]. Liquid biofuels (e.g., ethanol and butanol) offer significant advantages in comparison with gas products (H_2 and CH_4), which include a high energy intensity and easy storage and transportation [4]. Among them, medium-chain fatty acids (e.g., caproate (C6) and caprylate (C8)), which possess a chain of 6 to 12 carbons and a lower oxygen/carbon ratio than acetate and ethanol, are generally regarded as more valuable industrial commodities and more suitable precursors for liquid biofuels or biochemicals. Therefore, other than a valorisation process, the conversion of organic wastes to fatty acids also represents an important alternative to deal with the growing global energy demand.

However, direct and complete biological conversion of organic wastes is difficult due to the significant amount of non-biodegradable matter contained, such as lignin which accounts for 10-35% of the entire biomass [5-7]. The lignin content of biomass could be effectively utilized through gasification, which is commonly practiced for resource recovery and yields synthetic gas (syngas) as a mixture of H_2, CO, and CO_2. Syngas could then be used further as a feed stock for the production of useful biochemicals such as acetate and butyrate by either chemically-catalysed conversion (e.g., Fischer-Tropsch (FT) synthesis) or biological conversion routes (known as syngas fermentation) [8]. Nevertheless, FT synthesis is still not popularized and widely adopted due to its process complexity and relatively low efficiency. In contrast, biologically-catalysed generation of liquid biofuels or biochemicals via syngas fermentation is more efficient and requires less energy input [9]. Other merits include a higher tolerance for impurities such as sulfur compounds, a wider range of usable H_2, CO, and CO_2 mixture, and a lower operating temperature and pressure [10].

So far, the production of acetate from syngas (e.g., CO_2 and H_2) has been well studied [11-13], and the produced acetate could be converted to longer carboxylates such as butyrate and caproate through microbially-mediated chain elongation [14, 15]. Chain elongation is achieved through the reverse β-oxidation pathway, which includes acetate elongation to

butyrate via acetyl-CoA and butyrate elongation to caproate via butyl-CoA [15, 16]. *Clostridium kluyveri* is the best-known microbe capable of carrying out the well described reverse β-oxidation pathway [16-18]. Chain elongation processes not only add value to the final fermentation products but also improve their downstream processing, which remains a key issue to be addressed for syngas fermentation [1]. Pervaporation, electrodialysis, and solvent based extraction [19] are commonly proposed to refine the mixed products from syngas fermentation, and larger molecular weight products are generally more readily extracted and separated [20]. Chain elongation is therefore highly desired in order to reduce the operational cost associated with syngas fermentation.

One of the main challenges that restrict the application of syngas fermentation is the low solubility of hydrogen in the water phase as well as its poor gas-to-liquid mass transfer efficiency and rate [21], which govern the process rate. Mechanical augmentation such as gas circulation and liquid agitation could potentially promote the gas transfer process in fermentation reactors. However, these techniques are usually energy-intensive and faced with scale-up difficulties. The membrane biofilm reactor (MBfR) technology is particularly suitable for delivering gas with low solubility (e.g., H_2 and CH_4), which has been applied to hydrogen-based denitrification [22, 23] and methane-based denitrification [24-27], and could be utilized similarly for syngas fermentation. Since the gaseous substrate (i.e., syngas in this case) is supplied directly through gas-permeable and bubbleless membranes, its transfer could be enhanced greatly and controlled flexibly by pressure adjustment. Functional microorganisms could naturally attach to and proliferate on the membrane surface, and the produced fatty acids (e.g., C2, C4, and/or C6) could diffuse to the bulk liquid and be collected afterwards, as delineated in Figure 1. The decoupling of hydraulic retention time (HRT) and solid retention time (SRT) ensures a high biomass concentration, which also ensures good resilience of the MBfR to environmental changes. Proving this concept, Zhang

et al. [4, 13] observed high productions of fatty acids (C2, C4, and/or C6) in the MBfRs fed with syngas containing 60% H_2 and 40% CO_2. However, more work is of imperative need, in order to render a more comprehensive understanding of this technology as well as to better facilitate its future implementation.

Mathematical modeling serves as a useful and reliable tool to probe into emerging technologies and significantly reduces the workload related to process evaluation or optimization. To our knowledge, mathematical model is currently not available to describe syngas fermentation processes for fatty acids production, especially in MBfR systems. Therefore, in this work, we developed and tested a modelling approach which integrates multiple production pathways of fatty acids (i.e., C2, C4, and C6) using reported mixed culture experimental data obtained from a lab-scale MBfR fed with 60% H_2 and 40% CO_2. With the developed model, the impacts of key process parameters (i.e., gas supply and HRT) on the performance of the MBfR converting H_2/CO_2 to fatty acids were then investigated. The results of this work are expected to provide useful information for a better understanding and further applications of this MBfR technology for syngas fermentation.

MATERIALS AND METHODS

Model Development

Production of both short-chain and medium-chain fatty acids from H_2 and CO_2 by mixed microbial culture in a hollow-fiber MBfR has previously been demonstrated experimentally [4]. In the MBfR, H_2 and CO_2 were supplied through gas-permeable membranes, which also served as biofilm support, to the base of the biofilm, as shown in Figure 1. The hydrogen was for 100% utilized within the biofilms attached on the outer surface of the hollow-fiber membrane. Based on the experimental observations and the known metabolisms, Zhang et al.

[4] revealed the production of acetate, butyrate, and caproate from syngas containing 60% H_2 and 40% CO_2 could be described by Eqs. 1 to 4:

$$4H_2 + 2CO_2 \rightarrow C_2H_3O_2^- + H^+ + 2H_2O \text{ (at pH 7.0, } \Delta G^{0\prime} = -95 \text{ kJ mol}^{-1}) \quad (1)$$

$$C_2H_3O_2^- + 6H_2 + 2CO_2 \rightarrow C_4H_7O_2^- + 4H_2O \text{ (at pH 7.0, } \Delta G^{0\prime} = -143 \text{ kJ mol}^{-1}) \quad (2)$$

$$3C_2H_3O_2^- + 2H^+ + 4H_2 \rightarrow C_6H_{11}O_2^- + 4H_2O \text{ (at pH 7.0, } \Delta G^{0\prime} = -97 \text{ kJ mol}^{-1}) \quad (3)$$

$$C_4H_7O_2^- + 6H_2 + 2CO_2 \rightarrow C_6H_{11}O_2^- + 4H_2O \text{ (at pH 7.0, } \Delta G^{0\prime} = -143 \text{ kJ mol}^{-1}) \quad (4)$$

It should be noted that caproate could be elongated from either acetate (Eq. 3) or butyrate (Eq. 4) or both. However, the Gibbs free energy of Eq. 4 (-143 kJ mol^{-1}) is higher than that of Eq. 3 (-97 kJ mol^{-1}) [4], which means Eq. 4 would be favoured under same condition. This thermodynamic approach has been widely adopted to determine the most significant and feasible pathways involved in chain elongation [14, 16, 28]. Moreover, sequential chain elongation from acetate to caproate via butyrate has been well studied and clearly defined for *Clostridium kluyveri* [14, 29]. Therefore, for simplicity, chain elongation for caproate production was assumed to only follow Eq. 4 in this work. The biochemical reaction model was therefore developed based on the pathways indicated in Eqs. 1, 2, and 4. The possible ethanol production from CO_2 and H_2 was not included in the model due to the undetected ethanol concentration in the liquid phase of the experimental MBfR [4].

Given that most of the identified microorganisms dominating the biofilm of the experimental MBfR were affiliated with the genus of *Clostridium* (57.1%, based on the number of 16S rRNA gene clones) [4], which have been well categorized as capable of producing acetate, butyrate, and/or caproate from H_2 and CO_2, only one functional microorganism group was considered in the developed model. All with H_2 as the electron donor, the three biochemical reactions for fatty acids production (based on Eqs. 1, 2, and 4) were postulated to have the same yield, which links substrate consumption to biomass growth. This simplified approach could decrease the model complexity and avoid over-

parameterisation, and has been well accepted and widely applied to produce reliable results. Referring to Eqs. 1, 2, and 4, the molar H_2/CO_2 ratio of 3:2 in the syngas of the experimental MBfR meant that CO_2 was always in excessive supply, which was confirmed by the accumulated CO_2 content in the MBfR headspace [4]. Though an indispensable substrate, CO_2 was not included in the model, in view of its non-limiting effect on the fermentation processes. Monod equations were applied to describe the rate of each reaction, with non-competitive inhibition functions incorporated to depict the inhibition effects of non-substrate fatty acids. Eqs. 5, 6, and 7 show the Monod-based process rate equations for acetate (R_{Ac}), butyrate (R_{Bu}), and caproate (R_{Ca}) production, respectively. The stoichiometric relationships between substrates and products were formulated based on the characteristics of each reaction, with continuity checking performed to ensure correct mass balance of all components. The developed model integrates the relationships among four soluble species, i.e., hydrogen (S_{H2}), acetate (S_{Ac}), butyrate (S_{Bu}), and caproate (S_{Ca}), and two particulate species, i.e., functional biomass (X_B), and inert biomass (X_I). Table 1 lists the definitions, values, units, and sources of all parameters involved, while Table 2 details the stoichiometric and kinetic matrix of the developed model.

$$R_{Ac} = \mu_{Ac} \frac{S_{H2}}{K_{H2} + S_{H2}} \frac{K_{Ac}}{K_{Ac} + S_{Ac}} \frac{K_{Bu}}{K_{Bu} + S_{Bu}} X_B \quad (5)$$

$$R_{Bu} = \mu_{Bu} \frac{S_{H2}}{K_{H2} + S_{H2}} \frac{S_{Ac}}{K_{Ac} + S_{Ac}} \frac{K_{Bu}}{K_{Bu} + S_{Bu}} X_B \quad (6)$$

$$R_{Ca} = \mu_{Ca} \frac{S_{H2}}{K_{H2} + S_{H2}} \frac{S_{Bu}}{K_{Bu} + S_{Bu}} \frac{K_{Ac}}{K_{Ac} + S_{Ac}} X_B \quad (7)$$

where μ_{Ac}, μ_{Bu}, and μ_{Ca} are the maximum uptake rates for acetate, butyrate, and caproate production, respectively, and K_{H2}, K_{Ac}, and K_{Bu} are the hydrogen, acetate, and butyrate affinity constants, respectively.

Experimental Data Acquisition

The experimental data from the MBfR performing syngas fermentation reported by Zhang et al. [4] were used to test the developed model. The MBfR had a working volume of 2.4×10^{-4} m^3 and was inoculated with 4×10^{-5} m^3 mixed culture from a mesophilic methane production reactor. Syngas containing 60% H_2 and 40% CO_2 was fed constantly at 0.4 atm (inlet pressure) through gas-permeable hollow fibre membranes, the total surface area of which was 0.11 m^2. The MBfR was operated in batch mode with no continuous feeding flow to the bulk liquid during the experiment. The bulk liquid was continuously recirculated at 0.5 L min^{-1}. To inhibit the existence of methanogenesis, 10 mmol L^{-1} bromoethane sulfonate (BES) was initially added to the MBfR with pH manually controlled at 6.0 ± 0.2 with 2 M NaOH. The temperature was maintained at 35 ± 1 °C using a water bath. The composition of the bulk liquid is specified in Zhang et al. [4].

During the experiment, liquid samples were periodically taken from the MBfR to detect the cumulative contents of fatty acids and ethanol on a Gas Chromatograph (Agilent 7890, CA) equipped with a flame ionization detector and a 10 m × 0.53 mm HP-FFAP fused-silica capillary column. The contents of H_2, CO_2, and CH_4 in the headspace of the MBfR were determined on a Gas Chromatograph (Lunan model SP7890, CN) equipped with a thermal conductivity detector and a 1.5 m stainless steel column packed with 5 Å molecular sieve. More detailed information about the reactor operation and analytical methods could be found in Zhang et al. [4].

Model Testing and Simulations

The model was implemented on the software AQUASIM 2.1d [30] to simulate the MBfR for syngas fermentation. AQUASIM is equipped with functions of simulating the complicated microbial reactions and mass transfer processes in biofilm-based systems, and

has been proved capable of modeling real MBfRs [25, 27]. The MBfR was configured according to the experimental setup and modeled to consist of a completely mixed gas compartment (representing the membrane lumen operated) and a biofilm compartment (containing the biofilm and bulk liquid). The syngas supply to the biofilm was simulated through a diffusive link which connected the gas compartment to the base of the biofilm. The gaseous concentration of syngas in the gas compartment was jointly regulated by the gas flow rate and the gas pressure applied. The flux of syngas L from the gas to the biofilm matrix compartment through the membrane was modeled using the following equation.

$$L = k(\frac{S_g}{H} - S_l) \tag{8}$$

where S_g and S_l are the syngas concentrations in the gas and biofilm matrix compartments (g m^{-3}), respectively, k is the overall mass transfer coefficient (m d^{-1}), and H is the Henry's law constant (mole m^{-3} gas/mole m^{-3} liquid) [31].

Due to the reported unavailability of parameters related to chain elongation processes, the parameters associated with butyrate and caproate production, including μ_{Bu} (maximum uptake rate for butyrate production), μ_{Ca} (maximum uptake rate for caproate production), K_{Ac} (acetate affinity constant), and K_{Bu} (butyrate affinity constant), were estimated in this work, while the remaining parameters were directly adopted from Ni et al. [11]. This approach is generally acceptable and widely adopted for modeling research, and the model validity is ensured provided that a good match between experimental data and model predictions is obtained. The four parameter values were estimated through minimizing the sum of squares of the deviations between the experimental measurements and the model predictions for fatty acids production profiles including acetate, butyrate, and caproate. A sensitivity analysis was also carried out to evaluate the uncertainty of the four estimated parameters through generating response profiles of output to changes in parameter values.

The tested model was then applied to investigate the impacts of key process parameters (i.e., gas supply and HRT) on the performance of the MBfR converting H_2/CO_2 to fatty acids. HRT was defined as the average length of time that bulk liquid remained in the MBfR. HRT and syngas supply were varied over wide ranges (HRT: 0.25-8 days, syngas supply: 0.0001-0.012 m^3 d^{-1}) to investigate their effects on the total fatty acids production as well as the relative distribution of each species produced in the steady state of the MBfR. An average biofilm thickness was applied in the model without consideration of its variation with locations. Due to the production of microbial mass and the attachment of biomass particles, the biofilm thickness grew. Detachment of biomass at the biofilm surface to the bulk liquid was also described in the model to achieve the steady-state biofilm thickness. All simulations assumed an initial biofilm thickness of 5 μm which was irrelevant to the steady-state biofilm thickness [32] and were run for up to 100 days to reach steady state in terms of fatty acids production.

RESULTS AND DISCUSSION

Predicting Fatty Acids Production from H_2/CO_2 in the MBfR

The optimal set of parameter values was estimated using the AQUASIM built-in iterative algorithms, which minimize the residual error between experimental data and model predictions. The estimated values of the four parameters based on the experimental data in this work are presented in Table 1. μ_{Bu} and μ_{Ca} were obtained at 6.3 and 3.5 g COD g^{-1} COD d^{-1}, respectively, while K_{Ac} and K_{Bu} were estimated at 4500 and 2800 g COD m^{-3}, respectively. The fits of the model to the experimental data are visualized in Figure 2. Upon the commencement of the experiment, acetate appeared and accumulated, resulting in its growing concentration in the bulk liquid. Butyrate was only detected and kept increasing after a significant acetate accumulation. Similarly, the production of caproate only emerged at an

apparent butyrate accumulation. The model also captured the undetectable hydrogen concentration in the liquid phase of the experimental MBfR (data not shown). The good agreement between the measured data and model predictions ($R^2 \geq 0.8$) supported the validity of the developed model structure as well as the estimated parameters. Although the data used were limited, the main converting pathways were considered and the model fitting results proved satisfactory. The existing discrepancy between the experimental data and the model predictions (as shown in Figure 2) could likely be the result of the simplified model structure, i.e., a three-pathway model instead of a four-pathway model. The model could be further improved by including more potential pathways upon the advent of more and better experimental data of the MBfR performing syngas fermentation.

Uncertainty Analysis of the Key Model Parameters

A mathematical model usually involves a series of equations, input variables, and parameters, which are integrated to characterize processes under investigation. The uncertainty in the inputs are inevitably propagated to the model outputs. Therefore, parameter uncertainty of a model structure is of importance as it indicates which parameter combinations could be estimated under given measurement accuracy. Sensitivity analysis assesses how uncertainty in the outputs of a model can be apportioned to different sources of uncertainty in its inputs and is a useful tool to evaluate whether the values of theoretically identifiable parameters can be reliably obtained from experimental data. By taking into consideration the MBfR settings, an uncertainty analysis would gain a comprehensive understanding of the roles of parameters in the developed model structure.

To conduct the uncertainty analysis, the four kinetic parameters (μ_{Bu}, μ_{Ca}, K_{Ac}, and K_{Bu}) for fatty acids production were changed in the simulations one by one. The output sensitivities of model parameters to the fatty acids production calculated using best-fit

parameters are delineated in Figure 3. The base value of μ_{Bu} was 6.3 g COD g^{-1} COD d^{-1} with a range from 2.3 to 12.3 g COD g^{-1} COD d^{-1}. With the increasing value in μ_{Bu}, the production of acetate decreased while that of butyrate and caproate increased (Figure 3A). This change was attributed to the fact that more acetate produced was diverted to butyrate production at a higher μ_{Bu} (see process 2 in Table 2). A higher butyrate concentration also accelerated the concomitant production of caproate, for which butyrate is utilized as the precursor. An opposite trend was observed in terms of the response of fatty acids production to changes in the K_{Ac} value (Figure 3B), and such an effect was attributed to the inverse nature between μ_{Bu} and K_{Ac} in regulating the kinetic rate of butyrate production. With the increasing K_{Ac} value from 1500 to 7500 g COD m^{-3}, the production of butyrate was reduced, which led to less acetate consumption and less caproate formation from butyrate. As a result, the effluent caproate concentration dropped while the acetate production increased.

Figures 3C and 3D demonstrate the output sensitivities of μ_{Ca} (1.5-7.5 g COD g^{-1} COD d^{-1}) and K_{Bu} (1800-7800 g COD m^{-3}) to fatty acids production, respectively. An increase in μ_{Ca} resulted in a higher caproate production rate at the cost of a decreasing production of butyrate (Figure 3C). K_{Bu} had an impact on the production of butyrate and caproate in an opposite way (Figure 3D), which was associated with its different role from μ_{Ca} in determining the kinetic rate of caproate production from butyrate (see process 3 in Table 2). As shown in Figure 3C and 3D, the acetate production was not significantly affected by changes in either μ_{Ca} and K_{Bu} value.

Impacts of Operating Factors on the MBfR Performance

The development of an MBfR performing effective syngas fermentation processes is highly desirable, because it enables the practical production of valuable biochemicals from

waste materials. The model developed was therefore applied to investigate the improvement of the MBfR performance through controlling its syngas (H_2 and CO_2) supply and HRT.

Syngas supply directly determines the availability of substrates for syngas fermentation processes and serves as an important operational parameter of the MBfR. The impact of syngas supply on fatty acids production of the MBfR at HRT of 1 day is displayed in Figure 4A. The total fatty acids production increased while its rate decreased with the increasing syngas supply from 0.0001 to 0.012 m^3 d^{-1}. The finite biomass and syngas transfer to the biofilm via membranes to great extent limited the syngas conversion capacity of the MBfR, leading to the relatively slow growth in the total fatty acids production at syngas supply of more than 0.008 m^3 d^{-1}. The distribution of each fatty acid species was also influenced by syngas supply. As shown in Figure 4A, acetate was the dominant product species of syngas fermentation at syngas supply of 0.0001 m^3 d^{-1}, accounting for 97.8% of total fatty acids produced in terms of COD. This was the result of the competitive advantage of acetate production (process 1 in Table 2) for utilizing H_2 over the other two processes (processes 2 and 3 in Table 2) under limited syngas supply assessed, as evidenced by the dominant acetate accumulation rate shown in Figure 4B. Butyrate and caproate were also present in the outflow of the MBfR, taking up 2.1% and 0.1% of the total fatty acids production, respectively. Further increasing syngas supply provided more H_2 for processes 2 and 3 (Table 2), resulting in the increasing abundance of butyrate and caproate which reached 14.2% and 4.2%, respectively, at syngas supply of 0.012 m^3 d^{-1}. This was commensurate with the increasing butyrate and caproate accumulation rates in Figure 4B. Correspondingly, the production of acetate decreased gradually to 81.6% at syngas supply of 0.012 m^3 d^{-1}. These results revealed the key role played by syngas supply in regulating the syngas fermentation processes. However, single control over syngas supply seemed not sufficient for achieving chain elongation, considering the fact that under the operational conditions studied the

majority of the fatty acids produced were still short-chain fatty acids (i.e., acetate and butyrate), irrespective of the strength of syngas supply (see Figure 4A).

HRT is another key process parameter commonly used to manage performance of dynamic reactors or systems. Figure 4C shows the relationship between fatty acids production of the MBfR and HRT at steady state. Due to the fixed syngas supply at 0.002 m^3 d^{-1}, the total production of fatty acids was independent of HRT and remained almost constant at 0.5 g COD d^{-1}. However, the distribution of each fatty acid species was significantly affected by HRT. With the increasing HRT from 0.25 to 8 days, the fraction of acetate dropped gradually from 96.0% to 47.4% while that of caproate rose consistently from 0.2% to 29.4%. The fraction of butyrate first increased from 3.8% at HRT of 0.25 day and then remained about 23.0% at HRT of over 6 days. A longer HRT allowed more acetate produced to be further converted to butyrate and caproate, which greatly facilitated chain elongation processes. This was justified by the decreasing acetate accumulation rate and the increasing caproate accumulation rate when prolonging the HRT, as demonstrated in Figure 4D. Based on the trend in Figure 4C, the fraction of caproate was expected to continue increasing at HRT of more than 8 days. However, in Zhang et al. [13], acetate represented the major fermentation product with the coexistence of a low butyrate concentration but undetected caproate when the MBfR was operated at HRT of 9 days. This was different from our finding and might be ascribed to the different conditions applied (e.g., pH and syngas supply). Moreover, the MBfR in Zhang et al. [13] was not operated long enough to reach steady state, which could be another factor affecting the different reported compositions of fermentation products.

To sum up, the MBfR effectively performing mixed culture syngas fermentation could be achieved through controlling syngas supply and HRT using the developed model. From a practical point of view, a high HRT is imperative for chain elongation to produce a higher

proportion of medium-chain fatty acids with a higher value (e.g., caproate in this work) while a proper syngas supply should be provided to favour the speciation of syngas fermentation products as well as to fully exploit the conversion capacity of the MBfR. However, the obtained simulations of the MBfR in terms of syngas usage and fatty acids production under different operating conditions (Figure 4) only reflect the theoretical results at steady state, which require precise process control and might deviate from real applications. Moreover, the predictions might be highly dependent on the pathways considered for fatty acids production. The inclusion of other less favoured production pathways might to some extent affect the results. Though awaiting further experimental validation, the obtained information related to effective operation of the MBfR is expected to offer valuable guidance for operating practical systems taking on syngas fermentation processes and facilitate future experimentation of the MBfR technology for producing valuable biochemicals.

Future Applications and Development of the Model

This work proposed a modeling approach for mixed culture syngas fermentation in MBfR for the first time. This modeling approach, when integrated with a set of other powerful tools such as molecular approaches, isotopic studies, and measurements of reaction intermediates, will help reveal the detailed mechanisms of mixed culture syngas fermentation. The acquired biokinetics could be coupled with alcohol production from syngas fermentation [33] to yield a comprehensive model that is capable of describing in-situ biofuel production in the MBfR. However, the kinetic parameters in this work were estimated based on limited experimental data and might not be completely applicable to describing MBfRs performing syngas fermentation. Therefore, the validity of the developed model could be ameliorated when more experimental data under different operating conditions become available.

It's worth mentioning that in addition to H_2 and CO_2, CO represents another primary component of syngas produced via biomass gasification. CO could be converted to acetate, butyrate, and ethanol under anaerobic reducing conditions [34, 35], and fatty acids production from syngas containing H_2, CO_2, and CO has been proposed and proved [36, 37]. The developed model in this work could be expanded to include CO as a model substrate upon the advent of experimental MBfRs performing syngas fermentation from the more practical mixture of H_2, CO_2, and CO. As CO_2 was not taken into account as a limiting factor in the stoichiometric matrix as well as the Monod based process rate equations, the developed model could be further improved through the evaluation with scenarios considering different CO_2/H_2 ratios in the syngas composition.

CONCLUSIONS

A new modelling approach integrating multiple production pathways of fatty acids (including acetate, butyrate, and caproate) was developed and tested using reported mixed culture experimental data from a lab-scale MBfR fed with 60% H_2 and 40% CO_2, with the uncertainty of the key model parameters being evaluated. The results showed that the model well predicted the experimental data with reliable parameter values estimated. A high HRT is imperative for chain elongation to produce a higher proportion of caproate with a higher added value. A proper gas supply should be provided to favour the speciation of biological gas conversion products as well as to fully exploit the conversion capacity of the MBfR.

ACKNOWLEDGEMENTS

This study was supported by The University of Queensland Foundation Research Excellence Award. Xueming Chen acknowledges the scholarship support from China Scholarship Council (CSC). Dr. Bing-Jie Ni acknowledges the support of Australian

Research Council (ARC) Discovery Early Career Researcher Award (DE130100451) and ARC Discovery Project (DP130103147). The authors declare no competing financial interests.

REFERENCES

[1] D.J. Batstone, B. Virdis, The role of anaerobic digestion in the emerging energy economy, Current Opinion in Biotechnology 27 (2014) 142-149.

[2] K.J.J. Steinbusch, H.V.M. Hamelers, C.J.N. Buisman, Alcohol production through volatile fatty acids reduction with hydrogen as electron donor by mixed cultures, Water Research 42 (2008) 4059-4066.

[3] M.T. Agler, B.A. Wrenn, S.H. Zinder, L.T. Angenent, Waste to bioproduct conversion with undefined mixed cultures: the carboxylate platform, Trends in Biotechnology 29 (2011) 70-78.

[4] F. Zhang, J. Ding, Y. Zhang, M. Chen, Z.W. Ding, M.C.M. van Loosdrecht, R.J. Zeng, Fatty acids production from hydrogen and carbon dioxide by mixed culture in the membrane biofilm reactor, Water Research 47 (2013) 6122-6129.

[5] J. Daniell, M. Köpke, S. Simpson, Commercial Biomass Syngas Fermentation, Energies 5 (2012) 5372.

[6] X.M. Wang, J.M. Padgett, F.B. De la Cruz, M.A. Barlaz, Wood Biodegradation in Laboratory-Scale Landfills, Environmental Science & Technology 45 (2011) 6864-6871.

[7] C.N. Hamelinck, G. van Hooijdonk, A.P.C. Faaij, Ethanol from lignocellulosic biomass: techno-economic performance in short-, middle- and long-term, Biomass Bioenerg 28 (2005) 384-410.

[8] M. Yasin, Y. Jeong, S. Park, J. Jeong, E.Y. Lee, R.W. Lovitt, B.H. Kim, J. Lee, I.S. Chang, Microbial synthesis gas utilization and ways to resolve kinetic and mass-transfer limitations, Bioresource Technology 177 (2015) 361-374.

[9] A.M. Henstra, J. Sipma, A. Rinzema, A.J.M. Stams, Microbiology of synthesis gas fermentation for biofuel production, Current Opinion in Biotechnology 18 (2007) 200-206.

[10] H. Latif, A.A. Zeidan, A.T. Nielsen, K. Zengler, Trash to treasure: production of biofuels and commodity chemicals via syngas fermenting microorganisms, Current Opinion in Biotechnology 27 (2014) 79-87.

[11] B.J. Ni, H. Liu, Y.Q. Nie, R.J. Zeng, G.C. Du, J.A. Chen, H.Q. Yu, Coupling Glucose Fermentation and Homoacetogenesis for Elevated Acetate Production: Experimental and Mathematical Approaches, Biotechnology and Bioengineering 108 (2011) 345-353.

[12] S. de Kok, J. Meijer, M.C.M. van Loosdrecht, R. Kleerebezem, Impact of dissolved hydrogen partial pressure on mixed culture fermentations, Appl Microbiol Biotechnol 97 (2013) 2617-2625.

[13] F. Zhang, J. Ding, N. Shen, Y. Zhang, Z.W. Ding, K. Dai, R. Zeng, In situ hydrogen utilization for high fraction acetate production in mixed culture hollow-fiber membrane biofilm reactor, Appl Microbiol Biotechnol 97 (2013) 10233-10240.

[14] L.T. Angenent, H. Richter, W. Buckel, C.M. Spirito, K.J.J. Steinbusch, C.M. Plugge, D.P.B.T.B. Strik, T.I.M. Grootscholten, C.J.N. Buisman, H.V.M. Hamelers, Chain Elongation with Reactor Microbiomes: Open-Culture Biotechnology To Produce Biochemicals, Environmental Science & Technology 50 (2016) 2796-2810.

[15] K.J.J. Steinbusch, H.V.M. Hamelers, C.M. Plugge, C.J.N. Buisman, Biological formation of caproate and caprylate from acetate: fuel and chemical production from low grade biomass, Energy & Environmental Science 4 (2011) 216-224.

[16] C.M. Spirito, H. Richter, K. Rabaey, A.J.M. Stams, L.T. Angenent, Chain elongation in anaerobic reactor microbiomes to recover resources from waste, Current Opinion in Biotechnology 27 (2014) 115-122.

[17] T.I.M. Grootscholten, D.P.B.T.B. Strik, K.J.J. Steinbusch, C.J.N. Buisman, H.V.M. Hamelers, Two-stage medium chain fatty acid (MCFA) production from municipal solid waste and ethanol, Applied Energy 116 (2014) 223-229.

[18] S.J. Ge, J.G. Usack, C.M. Spirito, L.T. Angenent, Long-Term n-Caproic Acid Production from Yeast-Fermentation Beer in an Anaerobic Bioreactor with Continuous Product Extraction, Environmental Science & Technology 49 (2015) 8012-8021.

[19] H.-J. Huang, S. Ramaswamy, Overview of Biomass Conversion Processes and Separation and Purification Technologies in Biorefineries, in: S. Ramaswamy, H.-J. Huang, B.V. Ramarao (Eds.) Separation and Purification Technologies in Biorefineries, John Wiley & Sons, Ltd, Chichester, UK, 2013, pp. 1-36.

[20] M.T. Agler, C.M. Spirito, J.G. Usack, J.J. Werner, L.T. Angenent, Chain elongation with reactor microbiomes: upgrading dilute ethanol to medium-chain carboxylates, Energy & Environmental Science 5 (2012) 8189-8192.

[21] P.C. Munasinghe, S.K. Khanal, Biomass-derived syngas fermentation into biofuels: Opportunities and challenges, Bioresource Technology 101 (2010) 5013-5022.

[22] K.C. Lee, B.E. Rittmann, A novel hollow-fibre membrane biofilm reactor for autohydrogenotrophic denitrification of drinking water, Water Science and Technology 41 (2000) 219-226.

[23] K.C. Lee, B.E. Rittmann, Applying a novel autohydrogenotrophic hollow-fiber membrane biofilm reactor for denitrification of drinking water, Water Research 36 (2002) 2040-2052.

[24] Y. Shi, S. Hu, J. Lou, P. Lu, J. Keller, Z. Yuan, Nitrogen Removal from Wastewater by Coupling Anammox and Methane-Dependent Denitrification in a Membrane Biofilm Reactor, Environmental Science & Technology 47 (2013) 11577-11583.

[25] X. Chen, J. Guo, Y. Shi, S. Hu, Z. Yuan, B.-J. Ni, Modeling of Simultaneous Anaerobic Methane and Ammonium Oxidation in a Membrane Biofilm Reactor, Environmental Science & Technology 48 (2014) 9540-9547.

[26] C. Cai, S.H. Hu, J.H. Guo, Y. Shi, G.J. Xie, Z.G. Yuan, Nitrate reduction by denitrifying anaerobic methane oxidizing microorganisms can reach a practically useful rate, Water Research 87 (2015) 211-217.

[27] X. Chen, J. Guo, G.-J. Xie, Z. Yuan, B.-J. Ni, Achieving complete nitrogen removal by coupling nitritation-anammox and methane-dependent denitrification: A model-based study, Biotechnology and Bioengineering 113 (2016) 1035-1045.

[28] M. Coma, R. Vilchez-Vargas, H. Roume, R. Jauregui, D.H. Pieper, K. Rabaey, Product Diversity Linked to Substrate Usage in Chain Elongation by Mixed-Culture Fermentation, Environmental Science & Technology 50 (2016) 6467-6476.

[29] H. Seedorf, W.F. Fricke, B. Veith, H. Bruggemann, H. Liesegang, A. Strittimatter, M. Miethke, W. Buckel, J. Hinderberger, F.L. Li, C. Hagemeier, R.K. Thauer, G. Gottschalk, The genome of Clostridium kluyveri, a strict anaerobe with unique metabolic features, P Natl Acad Sci USA 105 (2008) 2128-2133.

[30] P. Reichert, AQUASIM 2.0-Computer program for the identification and simulation of aquatic systems, EAWAG, Dubendorf, Switzerland, 1998.

[31] R. Sander, Compilation of Henry's law constants (version 4.0) for water as solvent, Atmos Chem Phys 15 (2015) 4399-4981.

[32] A. Terada, S. Lackner, S. Tsuneda, B.F. Smets, Redox-stratification controlled biofilm (ReSCoBi) for completely autotrophic nitrogen removal: The effect of co- versus counter-diffusion on reactor performance, Biotechnology and Bioengineering 97 (2007) 40-51.

[33] J.M. Perez, H. Richter, S.E. Loftus, L.T. Angenent, Biocatalytic reduction of short-chain carboxylic acids into their corresponding alcohols with syngas fermentation, Biotechnology and Bioengineering 110 (2013) 1066-1077.

[34] K.M. Hurst, R.S. Lewis, Carbon monoxide partial pressure effects on the metabolic process of syngas fermentation, Biochemical Engineering Journal 48 (2010) 159-165.

[35] M. Kopke, C. Held, S. Hujer, H. Liesegang, A. Wiezer, A. Wollherr, A. Ehrenreich, W. Liebl, G. Gottschalk, P. Durre, Clostridium ljungdahlii represents a microbial production platform based on syngas, P Natl Acad Sci USA 107 (2010) 13087-13092.

[36] J.L. Gaddy, Producing acetic acid by creating a gas mixture of carbon monoxide, hydrogen, and carbon dioxide in a fermentation reactor containing an anaerobic bacteria that utilizes waste gas components and recover acetic acid from the aqueous phase, U.S. Patent No. 6340581, 2002.

[37] H. Younesi, G. Najafpour, A.R. Mohamed, Ethanol and acetate production from synthesis gas via fermentation processes using anaerobic bacterium, Clostridium ljungdahlii, Biochemical Engineering Journal 27 (2005) 110-119.

Table and Figure Legends

Table 1. Kinetic and Stoichiometric Parameters of the Developed Model

Table 2. Stoichiometric Matrix for the Developed Model

Figure 1. The schematic diagram of membrane biofilm reactor (MBfR) performing mixed culture syngas fermentation.

Figure 2. Model testing results based on the experimental data of the MBfR converting H_2 and CO_2 to fatty acids (measured data, symbols; model predictions, solid lines).

Figure 3. Output sensitivities of the four key model parameters to fatty acids production: **(A)** μ_{Bu}; **(B)** K_{Ac}; **(C)** μ_{Ca}; and **(D)** K_{Bu}.

Figure 4. Modeling results of the impacts of **(A and B)** syngas supply and **(C and D)** HRT on fatty acids production in the MBfR converting H_2 and CO_2 to fatty acids.

Table 1. Kinetic and Stoichiometric Parameters of the Developed Model

Parameter	Definition	Values	Unit	Source
Y	Yield coefficient for X_B	0.07	g COD g^{-1} COD	[11]
μ_{Ac}	Maximum uptake rate of X_B for acetate production	28.5	g COD g^{-1} COD d^{-1}	[11]
μ_{Bu}	Maximum uptake rate of X_B for butyrate production	6.3 ± 2.2	g COD g^{-1} COD d^{-1}	Estimated in this work
μ_{Ca}	Maximum uptake rate of X_B for caproate production	3.5 ± 0.8	g COD g^{-1} COD d^{-1}	Estimated in this work
k_{dec}	Decay rate coefficient of X_B	0.015	d^{-1}	[11]
K_{H2}	S_{H2} affinity constant for X_B	0.037	g COD m^{-3}	[11]
K_{Ac}	S_{Ac} affinity constant for X_B	4500 ± 800	g COD m^{-3}	Estimated in this work
K_{Bu}	S_{Bu} affinity constant for X_B	2800 ± 100	g COD m^{-3}	Estimated in this work

Table 2. Stoichiometric Matrix for the Developed Model

i	Component process	S_{H2} COD	S_{Ac} COD	S_{Bu} COD	S_{Ca} COD	X_B COD	X_I COD	Process rate equations
1	Acetate production from CO_2 and H_2	-1	$1-Y$			Y		$\mu_{Ac}\frac{S_{H2}}{K_{H2}+S_{H2}}\frac{K_{Ac}}{K_{Ac}+S_{Ac}}\frac{K_{Bu}}{K_{Bu}+S_{Bu}}X_B$
2	Butyrate production from acetate and H_2	-1	$-\frac{2\cdot(1-Y)}{3}$	$\frac{5\cdot(1-Y)}{3}$		Y		$\mu_{Bu}\frac{S_{H2}}{K_{H2}+S_{H2}}\frac{S_{Ac}}{K_{Ac}+S_{Ac}}\frac{K_{Bu}}{K_{Bu}+S_{Bu}}X_B$
3	Caproate production from of butyrate and H_2	-1		$-\frac{5\cdot(1-Y)}{3}$	$\frac{8\cdot(1-Y)}{3}$	Y		$\mu_{Ca}\frac{S_{H2}}{K_{H2}+S_{H2}}\frac{S_{Bu}}{K_{Bu}+S_{Bu}}\frac{K_{Ac}}{K_{Ac}+S_{Ac}}X_B$
4	Decay of X_B					-1	1	$k_{dec}X_B$

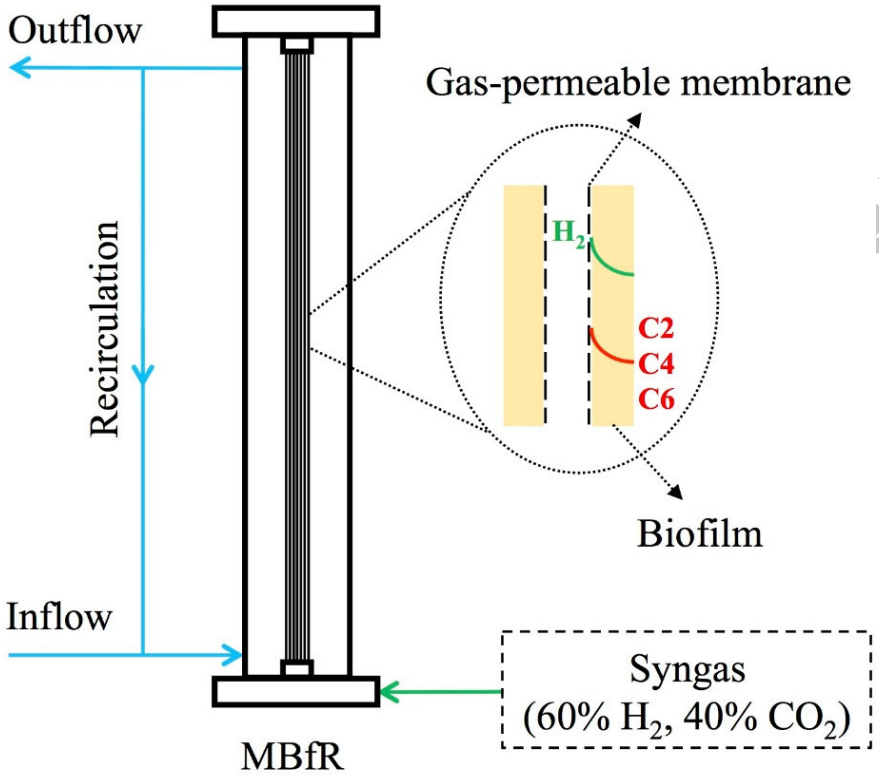

Figure 1. The schematic diagram of membrane biofilm reactor (MBfR) performing mixed culture syngas fermentation.

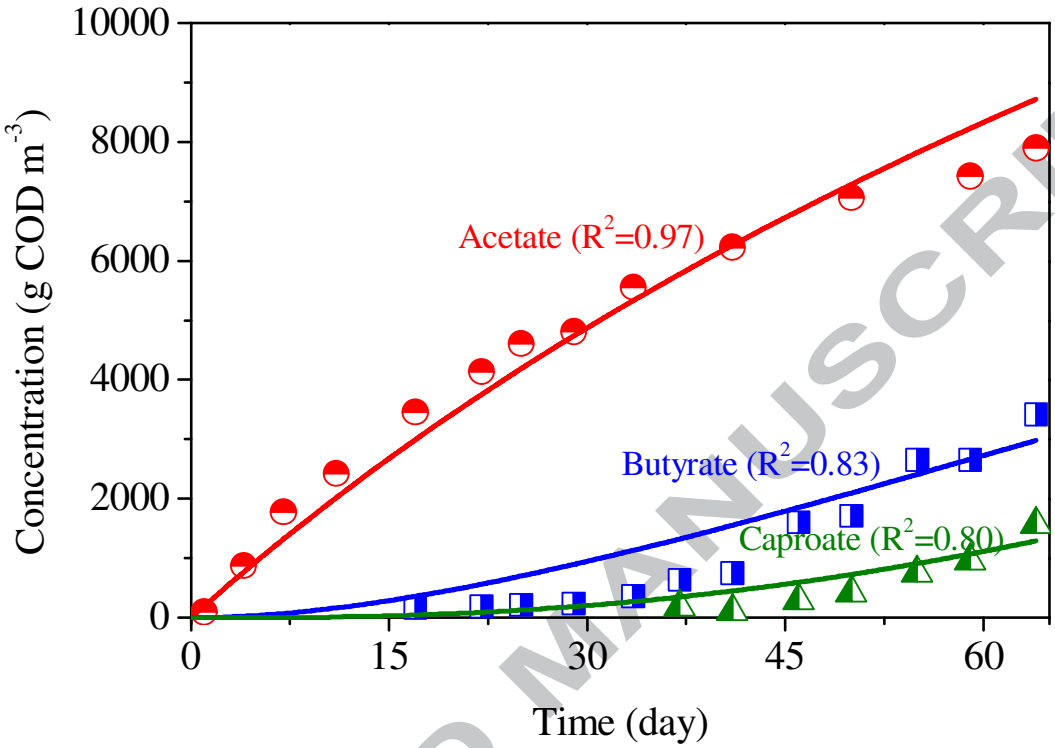

Figure 2. Model testing results based on the experimental data of the MBfR converting H_2 and CO_2 to fatty acids (measured data, symbols; model predictions, solid lines).

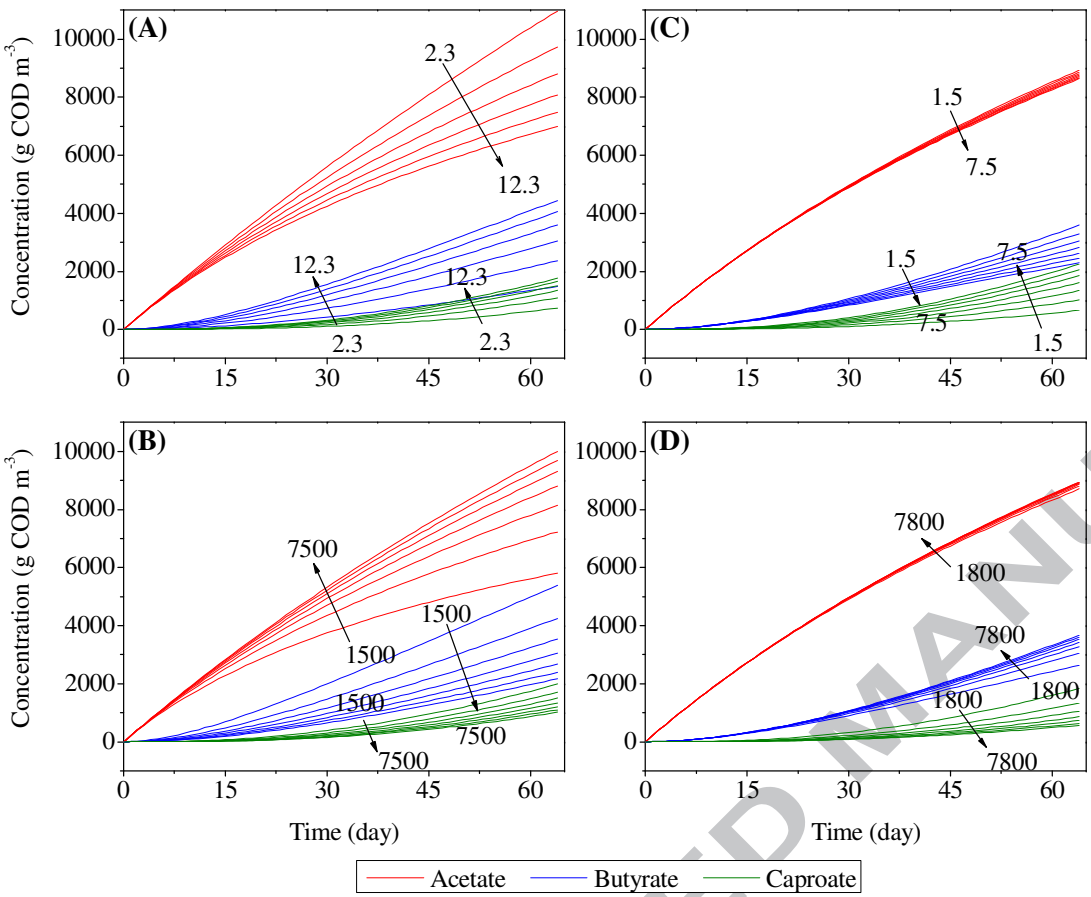

Figure 3. Output sensitivities of the four key model parameters to fatty acids production: **(A)** μ_{Bu}; **(B)** K_{Ac}; **(C)** μ_{Ca}; and **(D)** K_{Bu}.

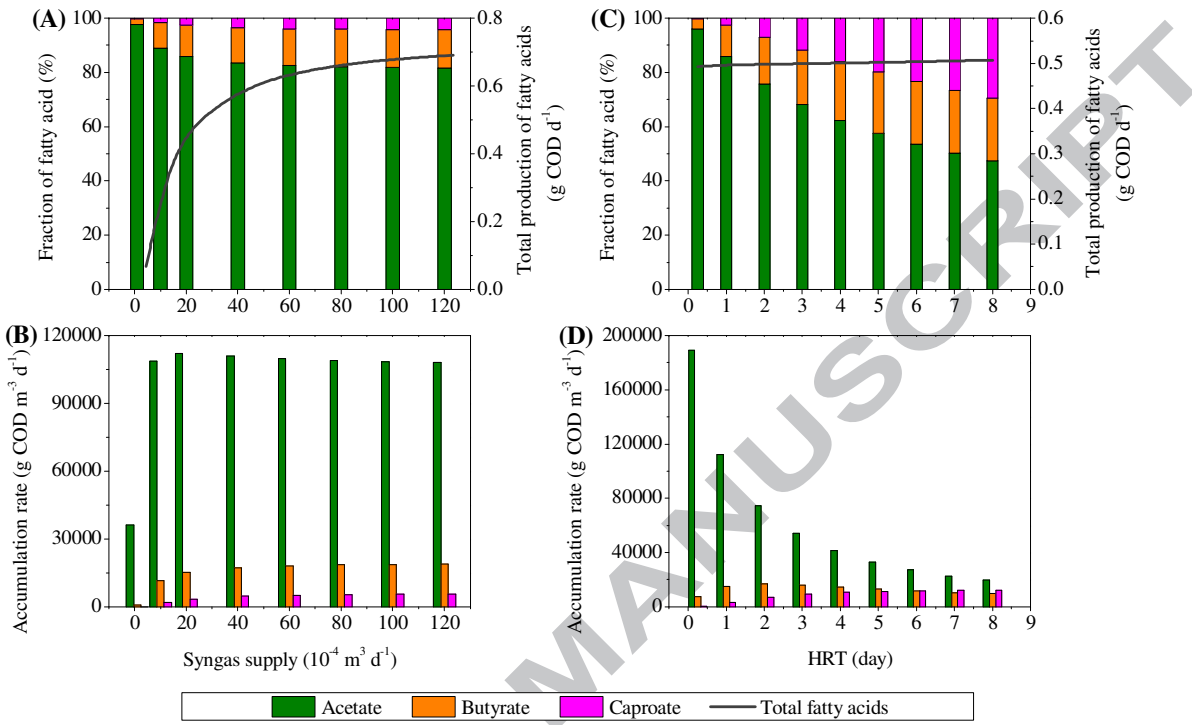

Figure 4. Modeling results of the impacts of **(A and B)** syngas supply and **(C and D)** HRT on fatty acids production in the MBfR converting H_2 and CO_2 to fatty acids.

Highlights

- A new model for syngas fermentation in MBfR was proposed and tested.
- Uncertainty of the four estimated parameters was explored by sensitivity analysis.
- Impacts of key process parameters on MBfR performance were assessed.